Journal of Sound and Vibration 328 (2009) 71–84

Contents lists available at ScienceDirect

Journal of Sound and Vibration

journal homepage: www.elsevier.com/locate/jsvi

Identification of structural damping in time domain

X.Y. Li, S.S. Law *

Civil and Structural Engineering Department, Hong Kong Polytechnic University, Hunghom, Kowloon, Hong Kong, People's Republic of China

ARTICLE INFO

Article history:
Received 2 June 2009
Received in revised form
20 July 2009
Accepted 30 July 2009
Handling Editor: L.G. Tham
Available online 20 August 2009

ABSTRACT

A structural damping identification procedure is proposed based on the sensitivity of acceleration response of the analytical model with model updating technique making use of the measured acceleration response. The viscous damping model obtained from the inverse modal transformation is adopted. The time-varying sensitivity matrix is computed by the Newmark method. Numerical study with a three-dimensional five-bay frame structure subjected to support excitation and a one-storey plane frame structure is performed to demonstrate the efficiency and validity of the proposed method. The effect of different sampling rates is studied. The damping ratios can be identified accurately from two "measured" acceleration responses with a high level of measurement white noise as well as model errors in the analytical model. The same procedure is later shown to be able to monitor the damping ratios of a time-varying system using moving windows of data in the identification with satisfactory results.

1. Introduction

It is essential to have an accurate dynamic model in the advanced research areas of structural dynamics such as fault diagnosis, real-time monitoring of structure, response prediction, load identification, etc. Due to the complexity of large engineering structures and the existence of measurement error, the dynamic characteristics of a system obtained from theoretical calculation and practical measurement may be quite different. In spite of a large amount of research, the understanding of the damping mechanisms is still primitive. A well known damping model usually called the "viscous damping", was first introduced by Rayleigh [1]. Rayleigh further idealized the damping matrix to be a linear combination of the mass and stiffness matrices, and this idealized model has since been commonly known as "Rayleigh damping", "proportional damping" or "classical damping".

Modal damping is often used in structural dynamics and it is considered as proportional damping for simplicity. However, the selection of the proportional coefficients still depends on engineering experience. Characterization of the damping forces in a vibrating structure has been an active area of research. A large body of literature can be found on damping since the publication of Lord Rayleigh's classic monograph "Theory of Sound" [1]. Modal damping ratio of a structure can be identified or estimated from test data by methods of parameter identification in both the time domain and frequency domain. Methods of the frequency domain [2,3] include half-power bandwidth method, peak picking method, admittance circle method, etc. Methods in the time domain include logarithmic-decrement method, ITD method [4,5], the eigensystem realization algorithm [6], STD method [7], derivatives of the ARMA method [8,9], the random decrement technique [10], weighted response-integral method [11], etc. Further developments include the wavelet transforms [12,13] and EMD-HT method [14,15].

* Corresponding author.
E-mail address: cesslaw@polyu.edu.hk (S.S. Law).

0022-460X/$ - see front matter © 2009 Elsevier Ltd. All rights reserved.
doi:10.1016/j.jsv.2009.07.033

Damping ratio, when compared with other parameters like the natural frequencies or mode shape, cannot be identified with high accuracy with existing methods, especially when the test data is contaminated with noise [3]. Method on how to improve the accuracy of identification is the focus of many current researches. Traditional modal-based method is difficult to identify the damping of the high frequency modes because these modes are difficult to excite. Kang et al [16] modeled the problem with Rayleigh damping and the two coefficients were identified from acceleration responses with 8 percent measurement noise. This damping model has the benefit of a small number of unknowns at the expense of poor representation of the damping of the structure. Shin and Oh [17] modeled the damping as viscous in their identification with acceleration responses polluted with 5 percent noise. The identified results depend on the initial assumed values with large oscillations. These existing methods have the limitations of not able to handle a large number of unknowns and with large measurement noise.

Lu and Law [18] have derived the sensitivity matrix of acceleration response with respect to a system parameter analytically for damage identification using responses from a few measurement locations. This paper identifies the damping ratio directly using the sensitivity of the acceleration responses in the time domain. The method could lead to high accuracy of identification in the damping ratios since the method is deterministic and the acceleration response is highly sensitive to damping ratios.

The sensitivity of acceleration response with respect to damping parameter is derived based on the normal mode damping model and it is obtained by a numerical approach such as the time-stepping integral method. The sensitivity matrix is time-varying and data sets from different time instances may be used. A numerical study using a three-dimensional five-bay frame structure and a one-storey plane frame structure is performed to demonstrate the efficiency and validity of the proposed method. The damping parameter can be identified accurately from two "measured" acceleration responses with a high level of noise as well as local errors in the analytical structural model. The same technique is further applied to a structure with time-varying damping properties with moving windows of data to have satisfactory results.

2. Sensitivity of acceleration response

The equation of motion of a N degrees-of-freedom (dofs) damped structural system under support excitation is given as

$$\mathbf{M}\ddot{\mathbf{x}}(\mathbf{t}) + \mathbf{C}\dot{\mathbf{x}}(t) + \mathbf{K}\mathbf{x}(t) = -\mathbf{M}\cdot\mathbf{L}\cdot\ddot{\mathbf{x}}_{\mathbf{S}}(\mathbf{t}) \tag{1}$$

where $\mathbf{M}$, $\mathbf{C}$ and $\mathbf{K}$ are the mass, damping and stiffness matrix, respectively. $\mathbf{L}$ is the mapping vector relating the DOFs with the force input to the corresponding DOFs of the system. Responses $\mathbf{x}$, $\dot{\mathbf{x}}$, $\ddot{\mathbf{x}}$ are the $N\times 1$ displacement, velocity, acceleration vectors, respectively. $\ddot{\mathbf{x}}_{\mathbf{S}}(\mathbf{t})$ is the support acceleration. $\mathbf{x}$, $\dot{\mathbf{x}}$, $\ddot{\mathbf{x}}$ can be computed from Eq. (1) using the Newmark method [19].

The system is assumed to exhibit normal modes and the viscous damping matrix $\mathbf{C}$ can be formed by the inverse modal transformation method [20] as

$$\mathbf{C} = (\mathbf{\Phi}^{\mathrm{T}})^{-1}\begin{bmatrix} \ddots & & \\ & 2\xi_j\omega_j & \\ & & \ddots \end{bmatrix}\mathbf{\Phi}^{-1} \tag{2}$$

where $\mathbf{\Phi}$ is the mode shape matrix, ξ_j and ω_j are the damping ratio and angular frequency for the ith mode of the structure. The second term on the right-hand side of Eq. (2) is a diagonal matrix.

Taking the first differential to both sides of Eq. (1) with respect to the damping ratio modeled as Eq. (2), we have

$$\mathbf{M}\frac{\partial\ddot{\mathbf{x}}}{\partial\xi_j} + \mathbf{C}\frac{\partial\dot{\mathbf{x}}}{\partial\xi_j} + \mathbf{K}\frac{\partial\mathbf{x}}{\partial\xi_j} = -\frac{\partial\mathbf{C}}{\partial\xi_j}\dot{\mathbf{x}} \tag{3}$$

The sensitivity of the damping matrix $\mathbf{C}$ can be computed from Eq. (2) as

$$\frac{\partial\mathbf{C}}{\partial\xi_j} = (\mathbf{\Phi}^{\mathrm{T}})^{-1}\begin{bmatrix} 0 & & \\ & 2\omega_j & \\ & & 0 \end{bmatrix}\mathbf{\Phi}^{-1} \tag{4}$$

The sensitivity of acceleration response with respect to the damping ratios, $\partial\ddot{\mathbf{x}}/\partial\xi_j$, can also be computed from Eqs. (1) and (3) using the Newmark method. The sensitivity matrix at time $\mathbf{t}$ can then be obtained as

$$\mathbf{S}(\mathbf{t}) = \begin{bmatrix} \frac{\partial\ddot{x}_l(t_1)}{\partial\xi_1} & \frac{\partial\ddot{x}_l(t_1)}{\partial\xi_2} & \cdots & \frac{\partial\ddot{x}_l(t_1)}{\partial\xi_m} \\ \frac{\partial\ddot{x}_l(t_2)}{\partial\xi_1} & \frac{\partial\ddot{x}_l(t_2)}{\partial\xi_2} & \cdots & \frac{\partial\ddot{x}_l(t_2)}{\partial\xi_m} \\ \cdots & \cdots & \cdots & \cdots \\ \frac{\partial\ddot{x}_l(t_{nt})}{\partial\xi_1} & \frac{\partial\ddot{x}_l(t_{nt})}{\partial\xi_2} & \cdots & \frac{\partial\ddot{x}_l(t_{nt})}{\partial\xi_m} \end{bmatrix} \tag{5}$$

where $\mathbf{t} = [t_1 \ t_2 \ \cdots \ t_{nt}]^{\mathrm{T}}$, nt is the number of time instances used, m is the number of modes considered, l denotes the DOF of the measurement and more than one measurement location can be used. The vector $\mathbf{t}$ can have equal or not equal time duration between its neighboring elements.

3. Damping identification by model updating

Neglecting higher order terms in the Taylor series expansion, the damping identification equation is obtained as

$$\mathbf{S}(\mathbf{t}) \cdot \Delta\xi(\mathbf{t}) = \Delta\ddot{\mathbf{x}}(\mathbf{t}) = \ddot{\mathbf{x}}_l^m(\mathbf{t}) - \ddot{\mathbf{x}}_l^i(\mathbf{t}) \tag{6}$$

where $\Delta\xi(\mathbf{t}) = \xi^u(\mathbf{t}) - \xi^i(\mathbf{t})$ is the augmented damping vector with m modes of the system at time t. The superscripts i, u and m denote the initial value, the updated value and the measured value, respectively. $\ddot{\mathbf{x}}_l^m(\mathbf{t})$ and $\ddot{\mathbf{x}}_l^i(\mathbf{t})$ are vectors of the acceleration response at the lth DOF from measurement and computation with the initial damping parameters, respectively.

An iterative approach is adopted to obtain $\Delta\xi(\mathbf{t})$ from Eq. (6) with the aim to reduce the error introduced by the Taylor series first-order approximation. An estimate on the response can be expressed as

$$\ddot{\mathbf{x}}_l^m(\xi^m, \mathbf{t}) = \ddot{\mathbf{x}}_l^i(\xi^i, \mathbf{t}) + \mathbf{S}(\xi^i, \mathbf{t}) \cdot \Delta\xi^1 + \mathbf{S}(\xi^1, \mathbf{t}) \cdot \Delta\xi^2 + \cdots + \mathbf{S}(\xi^{n-1}, \mathbf{t}) \cdot \Delta\xi^n \tag{7}$$

where the final identified damping ratio is $\xi^n = \xi^i + \Delta\xi^1 + \cdots + \Delta\xi^n$. The damping ratio ξ^k is assumed constant over the range of data for the identification in the following simulation studies. The iterative approach can be expressed as:

Step 1: For the initial analytical model, the identification equation is written as $\mathbf{S}(\xi^i, \mathbf{t}) \cdot \Delta\xi(\mathbf{t}) = \ddot{\mathbf{x}}_l^m(\xi^m, \mathbf{t}) - \ddot{\mathbf{x}}_l^i(\xi^i, \mathbf{t})$. $\Delta\xi^1$ can be computed from the equation for $k = 1$.

Step 2: The damping parameter vector ξ is updated as $\xi^k = \xi^i + \Delta\xi^k$. The damping vector ξ^i is updated as ξ^k and substituted into the analytical model. New sensitivity matrix $\mathbf{S}(\xi^k, \mathbf{t})$ is computed again, and the identification equation becomes $\mathbf{S}(\xi^k, \mathbf{t}) \cdot \Delta\xi(\mathbf{t}) = \ddot{\mathbf{x}}_l^m(\xi^m, \mathbf{t}) - \ddot{\mathbf{x}}_l^i(\xi^i, \mathbf{t}) - \mathbf{S}(\xi^i, \mathbf{t}) \cdot \Delta\xi^k$. $\Delta\xi^{k+1}$ can be computed from the equation again.

Step 3: The total number of iteration n is determined when both the following convergence criteria are met:

$$\frac{\|\ddot{\mathbf{x}}_l^{k+1} - \ddot{\mathbf{x}}_l^k\|}{\|\ddot{\mathbf{x}}_l^{k+1}\|} \le toler\ 1, \quad \frac{\|\xi^{k+1} - \xi^k\|}{\|\xi^{k+1}\|} \le toler\ 2 \tag{8}$$

where *toler* 1 and *toler* 2 are small prescribed values. They are taken as 10^{-6} in the following studies. $\ddot{\mathbf{x}}_l^k = \ddot{\mathbf{x}}_l(\xi^k)$ is the acceleration response computed from the structure with the damping parameter ξ^k. If these criteria are met, the iterative process stops. Otherwise, the damping vector is updated as $\xi^{k+1} = \xi^k + \Delta\xi^2 = \xi^i + \Delta\xi^k + \Delta\xi^{k+1}$. Put $k = k + 1$, and the computation go backs to Step 2 and repeats until convergence is reached.

4. Simulation study

4.1. A three-dimensional five-bay frame structure

A three-dimensional five-bay frame structure as shown in Fig. 1 serves for the numerical study. The finite element model consists of 37 three-dimensional Euler beam elements and 17 nodes. The length of all the horizontal, vertical and diagonal members between the centers of two adjacent nodes is exactly 0.5 m. The structure orientates horizontally and is fixed into a rigid support at three nodes at one end. Table 1 presents a summary of the main material and geometrical properties of the members of the frame structure. Each node has six DOFs, and altogether there are 102 DOFs for the whole structure.

The translational and rotational restraints at the supports are represented by large stiffnesses of 1.5×10^6 kN/m and 1.5×10^5 kN m/rad for Node 1, 1.7×10^9 kN/m and 1.7×10^8 kN m/rad for Node 7, 1.6×10^7 kN/m and 1.6×10^6 kN m/rad for Node 13 in six directions. The first 15 natural frequencies of the structure are presented in Table 2 with the fundamental

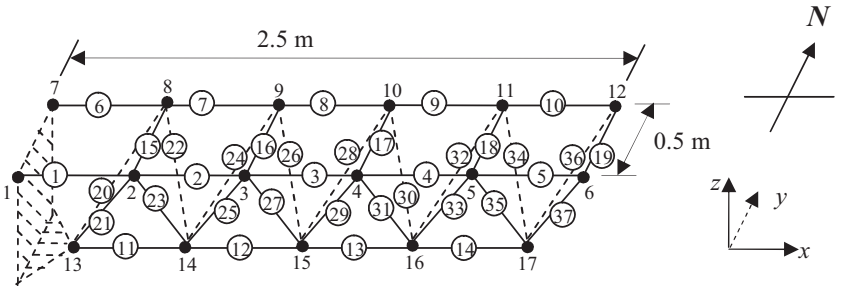

Fig. 1. A three-dimensional five-bay frame structure.

Table 1
Material and geometrical properties of members.

Properties	Member
Young modulus (N/m^2)	$2.10 \times 10^{+11}$
Area (m^2)	6.597×10^{-5}
Density (kg/m^3)	$1.2126 \times 10^{+4}$
Mass (kg)	0.32
Poisson ratio	0.3
Moment of area I_y (m^4)	3.645×10^{-9}
Moment of area I_z (m^4)	3.645×10^{-9}
Torsional rigidity J (m^4)	7.290×10^{-9}

Table 2
The vibration mode shapes.

Mode no.	Frequency (Hz)	Majority vibration motion
1	8.44	Torsional #1
2	15.91	Torsional #2
3	28.00	Vertical bending #1
4	34.04	Horizontal bending #1
5	49.05	Horizontal bending #2
6	70.78	Torsional #3
7	89.68	Torsional #4
8	131.09	Vertical bending #2
9	160.63	Horizontal bending #3
10	179.25	Axial #1
11	254.84	Axial #2
12	256.12	Vertical bending + axial #1
13	262.89	Vertical bending #3
14	265.02	Vertical bending + axial #2
15	280.57	Torsional #5

natural frequency at 8.44 Hz. The corresponding mode shapes are shown in Fig. 2 and Table 2 also gives a description on the nature of the vibration modes.

The major vertical bending modes are at Modes 3, 8 and 13 while the major axial modes are Modes 10, 11, 12 and 14 with very large axial motions in Modes 10 and 12. Modes 1, 2, 6, 7 and 15 exhibit very small motion in the lower chord of the frame and large horizontal motion in the upper chords leading to rotation of the frame cross-section about the lower chord. They are classified as the torsional modes. Modes 4, 5 and 9 are similar to the above modes but with large horizontal motion of the lower chord which is a characteristic of horizontal bending of the structure. Due to the asymmetry of the cross-section, the main component of the vibration modes is noted to be the torsional motion in the first 15 modes. The proportion of torsional motion in all six directions is the largest at 51.02 percent in the first mode and the smallest at 12.74 percent in the 14th mode.

4.2. Damping identification

The structure is subject to the El Centro ground motion in two directions as plotted in Fig. 3. Acceleration responses at Node 2 in y- and z-directions are used and they are believed to contain more of the strain energy in the vibration motion of the structure. The damping model in Eq. (2) is adopted with 4 percent damping ratio for each of the vibration modes in the computation of the dynamic response for the identification, while the initial value of all the damping ratios in the damping updating procedure is assumed to be 0.5 percent for each mode. Only the damping ratio of the first 15 modes will be identified. The sampling frequency is 2000 Hz and the responses recorded in one second are used for the damping identification with vector $\mathbf{t} = [0\ 1\ \ldots\ 1999] \cdot \Delta t$, where Δt is the time interval. The sensitivities of the acceleration response from Node 2 in y- or z-directions with respect to the damping ratios ξ_1, ξ_2 and ξ_3 are also computed from Eq. (3) by the Newmark method and they are shown in Fig. 4. Fig. 4 and other figures not shown indicates that the sensitivity increases with increasing mode number and the sensitivity time history is dominated with the frequency component of the structure, which can be explained by Eqs. (3) and (4). They are noted a few orders higher than the response sensitivities with respect to a system stiffness parameter as discussed in Ref. [18].

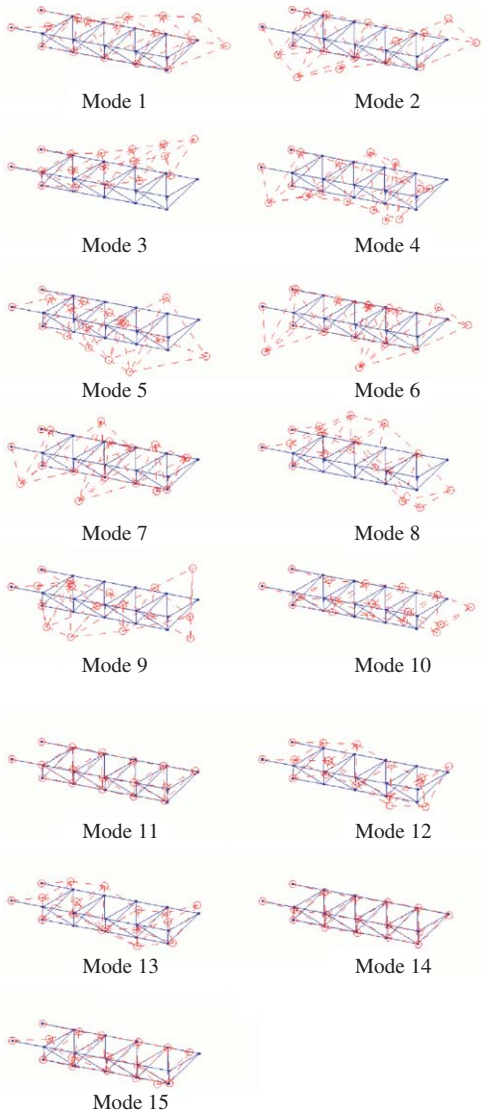

Fig. 2. Vibration mode shapes.

4.3. Scenarios for study

Different scenarios with measurement noise and model errors in the structure are investigated. White noise is added to the calculated responses to simulate the polluted measurements as follows:

$$\mathbf{R}_{\text{measured}} = \mathbf{R}_{\text{calculated}} + Ep * \mathbf{N}_{\text{oise}} * \text{var}(\mathbf{R}_{\text{calculated}}) \tag{9}$$

where $\mathbf{R}_{\text{measured}}$ is the vector of polluted responses; Ep is the noise level; N_{oise} is a standard normal distribution vector with zero mean and unit standard deviation; var(•) is the variance of the time history; $\mathbf{R}_{\text{calculated}}$ is the vector of calculated responses. Model error is introduced by stiffness changes modeled as a reduction in the elastic modulus of material, and they occur at the 16th, 26th and 27th element with 5, 10, and 10 percent reduction, respectively.

The different scenarios of damping identification are listed in the second row of Table 3 including:

(1) from calculated acceleration response only without measurement noise;
(2) from the calculated acceleration response contaminated with 5 percent noise;
(3) ditto with 10 percent noise;
(4) from calculated acceleration response of the structure with model error but without measurement noise;

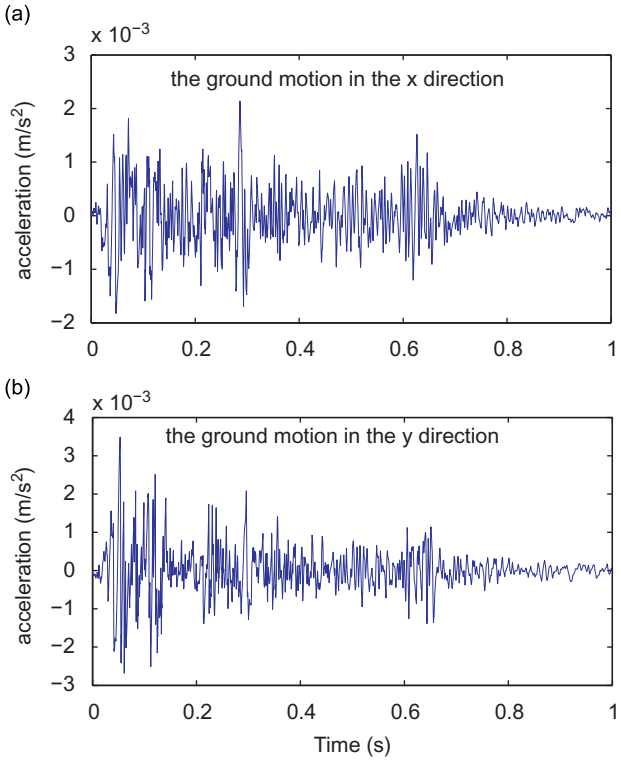

Fig. 3. The El Centro ground motion in *x*- and *y*-directions.

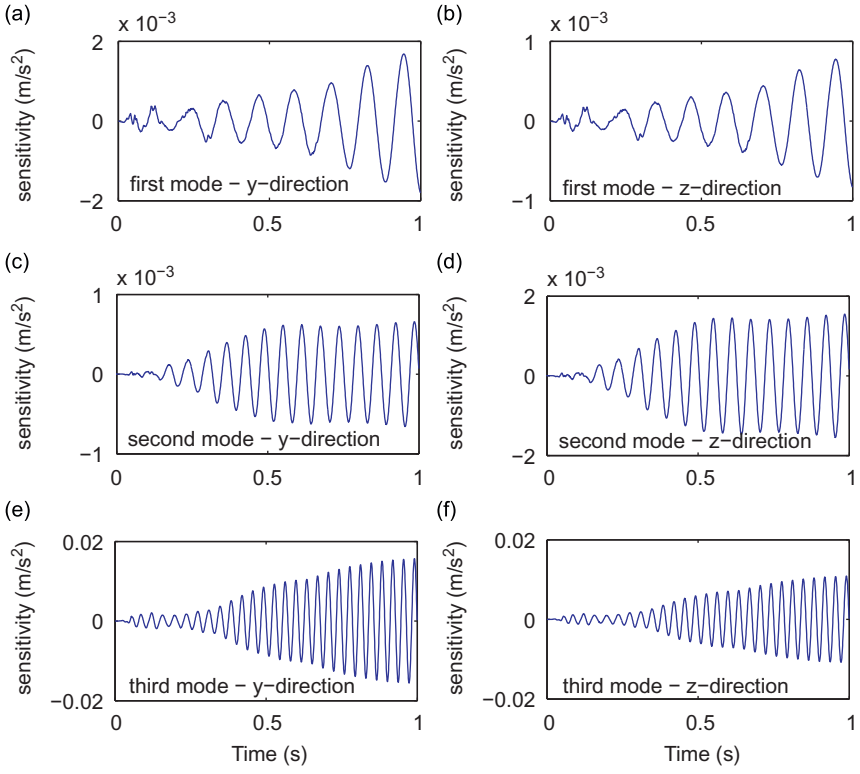

Fig. 4. Sensitivity of acceleration response with respect to damping ratio.

Table 3
The identified damping ratios (percent) and errors (percent) using measurements from Node 2.

Mode no.	Response from intact structure						Response from structure with local model errors							
	(1) W/o noise		(2) With 5 percent noise		(3) With 10 percent noise		(4) W/o noise		(5) With 5 percent noise		(6) With 10 percent noise		(7) With 20 percent noise	
	Value	Error	Value	Error	Value	Error	Value	Error	Value	Error	Value	Error	Value	Error
1	4.00	0.05	3.80	5.09	3.60	9.94	4.14	3.51	3.93	1.88	3.72	6.94	3.35	16.25
2	3.99	0.20	3.97	0.68	3.95	1.16	3.87	3.20	3.85	3.71	3.83	4.23	3.79	5.32
3	4.00	0.00	3.96	1.02	3.92	2.02	4.09	2.35	4.05	1.30	4.01	0.26	3.93	1.83
4	4.00	0.00	4.01	0.28	4.02	0.56	3.96	1.05	3.97	0.78	3.98	0.50	4.00	0.04
5	4.00	0.00	4.00	0.12	3.99	0.24	4.00	0.08	3.99	0.20	3.99	0.31	3.98	0.55
6	4.00	0.00	4.01	0.27	4.02	0.55	4.02	0.53	4.03	0.81	4.04	1.08	4.07	1.64
7	4.00	0.01	4.00	0.05	4.00	0.10	3.96	0.94	3.96	0.98	3.96	1.03	3.95	1.13
8	4.00	0.12	3.97	0.88	3.94	1.62	3.99	0.35	3.96	1.10	3.93	1.84	3.87	3.27
9	4.00	0.00	4.00	0.02	4.00	0.03	4.02	0.57	4.02	0.55	4.02	0.53	4.02	0.48
10	4.00	0.08	4.01	0.18	4.02	0.44	4.03	0.71	4.04	0.98	4.05	1.24	4.07	1.78
11	3.79	5.22	3.64	9.08	3.47	13.30	3.76	5.88	3.60	10.03	3.43	14.23	3.08	22.90
12	4.47	11.66	4.76	19.02	5.14	28.54	4.60	15.00	4.92	23.09	5.33	33.16	6.48	62.05
13	3.43	14.16	3.74	6.42	4.16	3.95	3.42	14.50	3.79	5.33	4.25	6.16	5.85	46.31
14	5.12	28.09	4.95	23.85	2.83	29.29	3.73	6.71	3.93	1.81	2.86	28.48	3.14	21.49
15	5.70	42.61	5.89	47.15	6.72	67.95	6.04	50.93	6.72	68.04	6.84	70.95	6.56	63.99

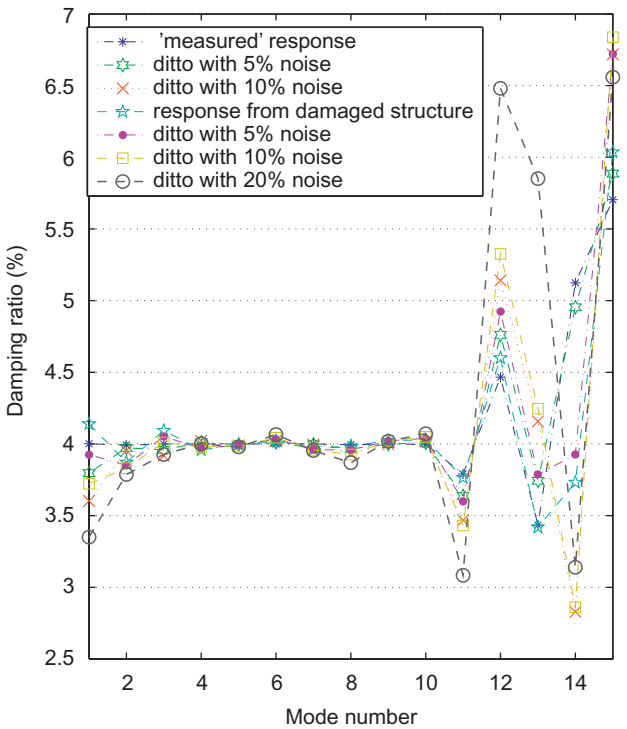

Fig. 5. The identified damping ratios.

(5) ditto with 5 percent noise;
(6) ditto with 10 percent noise;
(7) ditto with 20 percent noise.

The identified results for the above scenarios are presented in Table 3 and Fig. 5. Results in Column 3 show that the first 10 damping ratios are accurately identified with the largest error of 0.2 percent in the 2nd mode. However, for the 11th–15th damping ratios, the smallest error of 5.2 percent occurs at 11th mode and the largest error of 42.6 percent occurs in 15th mode. This can be explained by observing the mode participation factor and the Euclidean norm of the acceleration

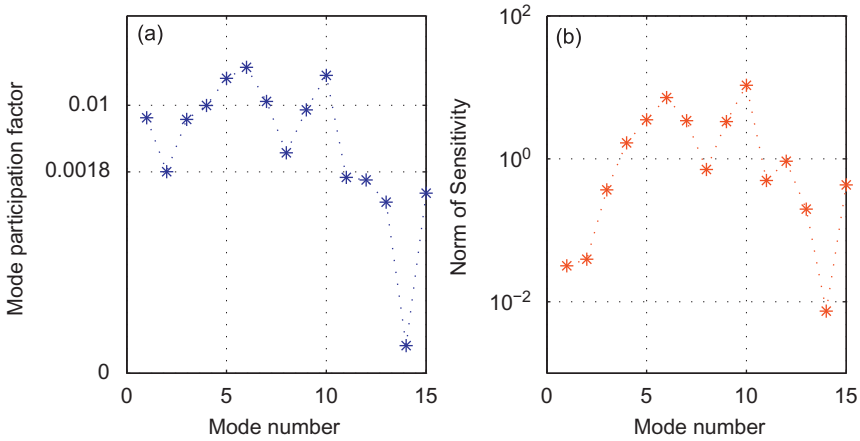

Fig. 6. The distribution of mode participation factor and the norm of acceleration sensitivity.

sensitivity vector shown in Fig. 6. The ith mode participation factor for the acceleration response measured from lDoF is computed from $\Phi_{li} \cdot q_i$, where Φ_{li} is the lth component of the ith mode shape Φ_i and q_i is the ith generalized coordinate of the structure under the given excitation. The mode participation factors of 11th–15th mode are relatively small compared with those of the first 10 modes and the sensitivity of the remaining five modes is also smaller than the preceding modes except the first three modes. In the first 10 modes, mode participations of 2nd and 8th mode are small and the corresponding errors in the third column of Table 3 are also larger. This shows that the mode participation affects greatly the accuracy of the damping identification. The small mode participation factor is caused by the geometry and the boundary condition of the structure as well as the frequency component of the support excitation. Other studies not shown indicate that even when sensors are placed at all free translational DOFs, relatively large errors still occur with the identified results at the 11th to 15th modes.

The first 15 damping ratios identified when 5 and 10 percent noise is included in the "measured" acceleration responses are also presented in Table 3. The error increases with the level of noise. The largest error in the first 10 modes is around 10 percent in the 1st mode. The largest error in the first 15 modes is about 68 percent in the 15th mode.

The accuracy of identification is also affected with the presence of model errors. The first 10 damping ratios are, however, acceptable with the largest error of 3.5 percent when there is no noise in the measurement. When there is 5, 10 or 20 percent noise included in the "measured" data, the identified damping ratios presented in Table 3 are also acceptable but with a marginal increase in the error of identification in the first 10 damping ratios. The above observations show that a relatively large motion in a vibration mode is needed for an accurate identification of its damping ratio.

To further check on the updating effect on the acceleration responses, a comparison between the accurate acceleration responses, the acceleration response calculated with the initial damping ratio and the final updated acceleration response with the identified damping ratios is made for the worst case with model errors and 20 percent noise in the "measured" acceleration response, and the results are shown in Fig. 7. The updated acceleration response in the y-direction matches the accurate response very well and is greatly improved from the calculated response at the beginning of model updating.

4.4. *Effect of sampling rate*

The effect of different sampling rate on the identified results is also studied with the "measured" acceleration response simulated from the analytical model with model errors and with 10 percent noise. Four different sampling rates are studied including 2000, 1000, 500, and 250 Hz. The first second data is used in the identification in Eq. (6), and the identified damping ratios for the first 15 modes are listed in Table 4 for comparison. The results for the first 10 modes are good with higher accuracy for higher sampling rates like 1000 and 2000 Hz. The error in the results for the last five modes is large irrespective of the sampling rates. Studies not shown also indicate that the accuracy of the identified results could be improved when more data points are used, but the difference of accuracy between the first 10 modes and the last five modes remains. For the same sampling frequency, enough number of data points can ensure the identification equation to be over-determined. Too many data points will affect the accuracy of damping identification, because some modes may have decayed to zero with time and these modes will have little contribution to the vibration of the structure.

It should be noted that the response obtained from Eq. (1) or from measurement contains components from all the structural vibration modes. A sampling of the response results in a subset of the response measurement according to the Nyquist criterion. The time domain approach does not mainly depend on the frequency information of the measured response as the frequency domain method, because it also makes use of the vibration amplitude in the solution process as from the following discussions.

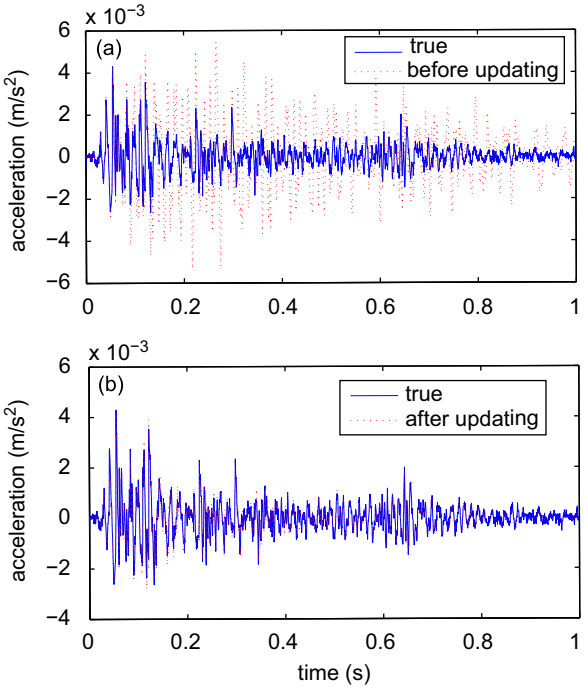

Fig. 7. Comparison of the *y*-acceleration response from Node 2.

Table 4
Identified damping ratios (percent) and errors (percent) from using different sampling rates.

Mode no.	Sampling rate							
	2000/*s*		1000/*s*		500/*s*		250/*s*	
	Value	Error	Value	Error	Value	Error	Value	Error
1	3.73	6.75	4.04	1.00	4.23	5.75	4.58	14.50
2	3.85	3.75	3.52	12.00	2.43	39.25	3.42	14.50
3	3.91	2.25	3.95	1.25	4.15	3.75	4.10	2.50
4	3.99	0.25	3.96	1.00	4.08	2.00	4.61	15.25
5	3.99	0.25	4.02	0.50	3.96	1.00	3.76	6.00
6	4.04	1.00	4.02	0.50	4.04	1.00	4.05	1.25
7	3.95	1.25	4.00	0.00	3.99	0.25	4.04	1.00
8	3.89	2.75	3.86	3.50	3.06	23.50	3.61	9.75
9	4.04	1.00	4.03	0.75	4.12	3.00	3.84	4.00
10	4.04	1.00	4.05	1.25	3.97	0.75	4.01	0.25
11	3.84	4.00	4.29	7.25	4.09	2.25	3.36	16.00
12	4.69	17.25	4.91	22.75	4.28	7.00	3.77	5.75
13	3.99	0.25	3.00	25.00	1.78	55.50	3.19	20.25
14	3.53	11.75	3.83	4.25	0.51	87.25	0.14	96.50
15	5.19	29.75	5.92	48.00	5.14	28.50	7.68	92.00
Total error	–	83.25	–	129.00	–	260.75	–	299.50

The amplitude of the structural response, when expressed in the form of Duhamel integral of

$$\sum_{i=1}^{n} \int \frac{e^{-\xi_i \omega_i \tau}}{\omega_{id}} \sin(\omega_{id}\tau) \cdot F(t-\tau)\,\mathrm{d}\tau$$

includes the structural information in the two terms of $\sin(\omega_{id}\tau)$ and $e^{-\xi_i\omega_i\tau}/\omega_{id}$. The Nyquist frequency has to be satisfied if the structural vibration information (both the amplitude and frequency) is sought from the term $\sin(\omega_{id}\tau)$. However, the term $e^{-\xi_n\omega_n\tau}$ is an exponential function and is independent of the sampling frequency. The time-domain method is therefore less dependent on the Nyquist frequency and the damping identification can be performed successfully with a low sampling rate.

4.5. One-storey plane frame structure

Another one-storey plane frame structure is also studied on the random results that may exist in the different modes. A sinusoidal excitation $F(t) = 10\ \sin(12\pi t)N$ is applied vertically at node 6 as shown in Fig. 8. The vertical acceleration at node 7 and the horizontal acceleration at node 10 is recorded for the study. The columns of the frame are 1.2 m high and the cross-beam is 0.6 m long, and each member has 10 mm depth and 20 mm breadth uniform rectangular cross-section. The modulus of elasticity and the mass density of materials are, respectively, $69 \times 10^9\ \mathrm{N/m^2}$ and $2700\ \mathrm{kg/m^3}$.

The finite element model of the structure consists of four and three equal beam-column elements in each vertical and horizontal member, respectively. The translational and rotational restraints at the supports are represented by large stiffnesses of 1.5×10^{10} kN/m, 1.5×10^9 kN/m and 1.5×10^7 kN m/rad, respectively. The damping model in Eq. (2) is adopted with 4 percent damping ratio for each of the vibration modes in the computation of the dynamic response for the identification, while the initial value of all the damping ratios in the damping updating procedure is assumed to be 0.5 percent for each mode. Only the damping ratio of the first 20 modes will be identified. The first 12 natural frequencies of the structure are 13.09, 57.29, 76.68, 152.38, 196.43, 227.28, 374.59, 382.42, 580.05, 699.10, 764.79 and 977.69 Hz. The sampling frequency is 2000 Hz which is high enough not to have computation error from using the Newmark method, and 0.25 s of measured data is used. 5 percent white noise is added to the calculated responses to simulate the polluted

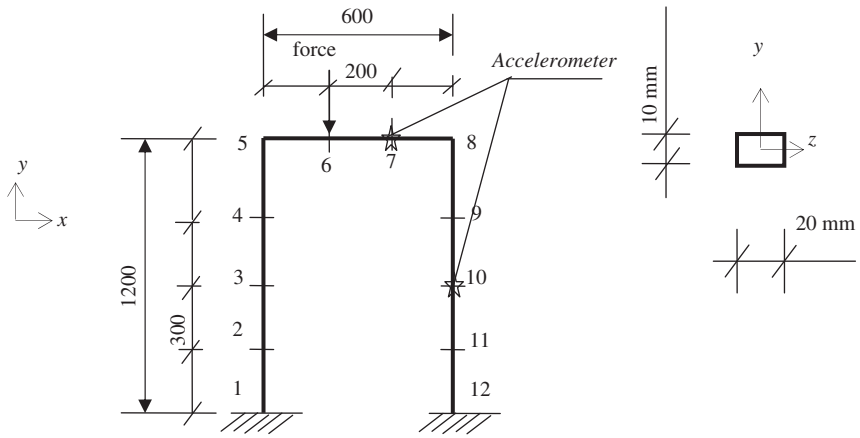

Fig. 8. A one-story plane frame structure.

Table 5
The identified damping ratios (percent) and errors (percent) of the one-story plane frame structure.

Mode no.	Response from intact structure		
	W/o noise		
	Modal participation factor	Value	Error
1	0.585	3.95	1.26
2	4.508	4.00	0.09
3	0.502	4.02	0.42
4	3.496	4.00	0.11
5	0.065	4.12	2.98
6	2.373	4.00	0.02
7	0.395	3.97	0.71
8	0.406	4.04	0.97
9	1.072	3.99	0.16
10	0.029	4.25	6.28
11	0.230	4.00	0.014
12	0.005	2.89	27.78
13	0.092	4.11	2.83
14	0.017	4.02	0.41
15	0.247	3.97	0.66
16	0.025	3.83	4.276
17	0.108	3.90	2.47
18	0.022	3.43	14.33
19	0.166	4.03	0.72
20	0.066	4.16	3.965

measurements as in Eq. (9). The identified damping ratios using the proposed method are presented in Table 5. The first 20 damping ratios can be obtained satisfactorily even with 5 percent noise in the measured responses. The largest error of 27.78 percent occurs at 12th mode. Further inspection show that modes 5, 10, 12, 13, 16, 17, 18 and 20 have the error of identification larger than 1 percent while they all have a modal participation factor equal or less than 1 percent. There is also no fixed pattern of variation in the results compared with that for the last structure indicating that the observation in last structure is mode dependent. The conclusion on the requirement of a large modal participation factor of the vibration mode for the last structure remains valid for this structure.

4.6. Identification of time-varying damping ratio

The truss structure studied previously is assumed to exhibit time-varying damping in the first five modes as shown in the second and third columns of Table 6 while the damping ratios for the other modes are assumed to be 4 percent. The time-varying damping ratio exhibit sudden changes at the time instances of 2 and 4 s. The initial damping ratio in the damping updating procedure is assumed to be 0.5 percent for each mode while only the damping ratio of the first 15 modes will be identified. The set of "measured" accelerations from Nodes 2 and 8 in the y- and z-directions are used in the identification.

A moving window of 1000 data points (data from 0.5 s) is extracted from the "measured" data at an increment of 50 data points, i.e. 0.025 s, and 7 s recorded acceleration data is used. There are 261 sets of windowed data. The proposed identification procedure is applied to each of these windowed data. The first five identified damping ratios are shown alongside with the true values over the measurement period in Figs. 9–13. The identified damping ratios for Modes 6–10 are fairly accurate but with large errors for Modes 11–15. The largest error averaged over the time duration in the former group of modes (Modes 6–10) is 6.14 percent in Mode 6. The identified time-varying damping ratios in Figs. 9–13 match the

Table 6
The results from time-varying damping model.

Mode no.	True		Identified	
	Duration (s)	Damping (Percent)	Duration (s)	Average damping (Percent)
1	0–2	4.0	0.25–1.75	4.02
	2–4	5.0	2.25–3.75	5.02
	4–7	5.5	4.25–6.75	5.49
2	0–2	4.0	0.25–1.75	3.95
	2–4	3.0	2.25–3.75	2.85
	4–7	3.5	4.25–6.75	3.39
3	0–2	4.0	0.25–1.75	4.06
	2–4	6.0	2.25–3.75	6.00
	4–7	5.5	4.25–6.75	5.55
4	0–2	4.0	0.25–1.75	3.97
	2–4	4.5	2.25–3.75	4.46
	4–7	5.5	4.25–6.75	5.46
5	0–2	4.0	0.25–1.75	4.00
	2–4	5.5	2.25–3.75	5.49
	4–7	6.5	4.25–6.75	6.48

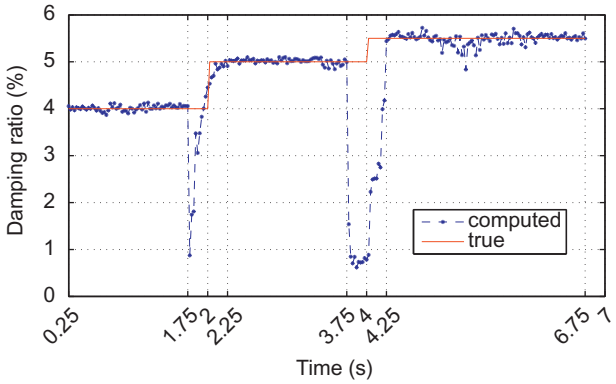

Fig. 9. Identified first damping ratio.

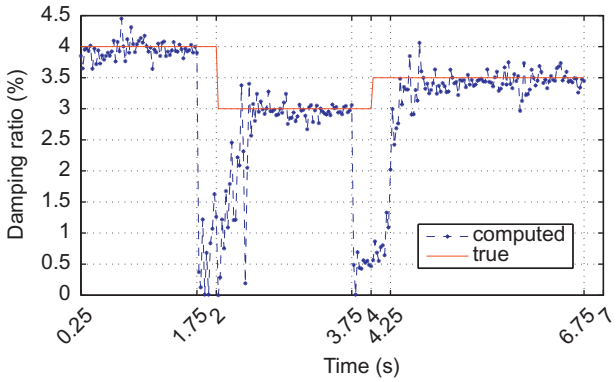

Fig. 10. Identified second damping ratio.

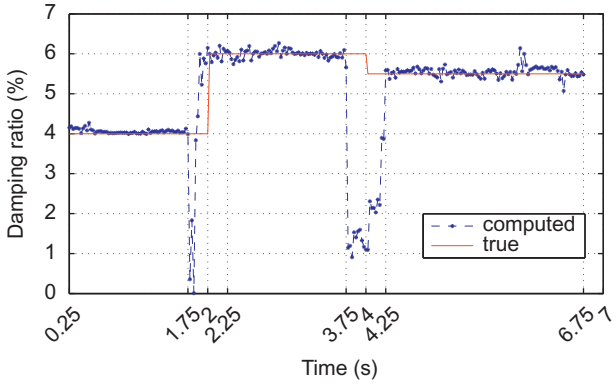

Fig. 11. Identified third damping ratio.

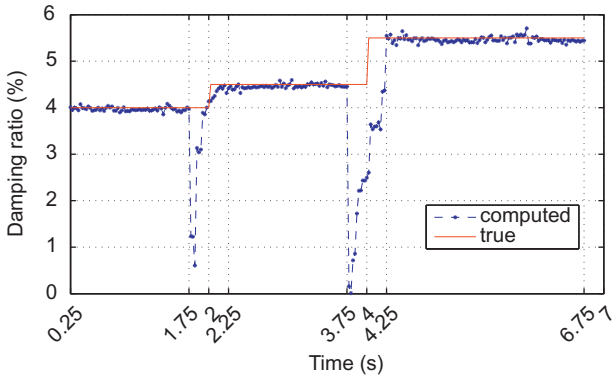

Fig. 12. Identified fourth damping ratio.

true ones basically with fluctuations around the mean value during the periods of constant damping ratios, and there are periods of sudden changes during the transition between two constant damping values. These features are observed in all the first five modes. The range of fluctuations is largest in the second identified modal damping. However, intervals with relatively stable values can be identified for each of the curves. If an average is taken over each of these intervals, they are very close to the true damping ratios as presented in the last column of Table 6.

It can be seen from all the curves on the identified damping values that the period with sudden changes lasts approximately 0.5 s. This is because 0.5 s of data has been used in each identification computation. If the whole window of data has a constant damping ratio, the identified damping value would be very close to the true one with fluctuations. However, when the windowed data comes from two consecutive periods with different damping ratios, the identified results would be in error. The above observations indicate that the periods with sudden changes can be shortened with the

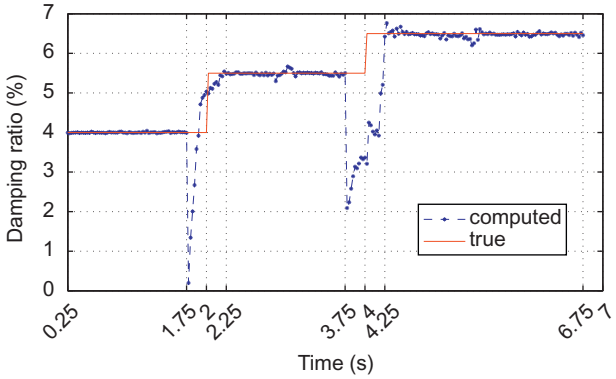

Fig. 13. Identified fifth damping ratio.

use of data from a shorter duration. This can be accomplished from using a short duration of data sampled at a high sampling rate or sampled from many sensors.

5. Discussions

Compared to other damping identification method, the proposed method has very strong ability in tolerating the measurement noise. The proposed method can identify simultaneously the damping ratio of a large number of vibration modes, while the traditional frequency domain method is difficult to identify the higher modes because these modes are difficult to excite. The proposed method also has the advantage of using very few sensors for measuring the acceleration responses to obtain the damping parameters.

Attempt has been made to identify both the structural damage and the damping ratio simultaneously using the sensitivity approach but fail. Inspection of Eq. (3) shows that the damping ratio is in fact coupled with the stiffness matrix via the mode shape matrix on the left-hand side of the equation. Therefore, the proposed method is only suitable for the identification of modal damping alone. Any error in the initial finite element model of the structure would lead to a less accurate set of results as presented in Table 3 and as discussed previously. The proposed method has the ability of identifying a highly accurate set of damping ratios which is robust to measurement noise and local model errors when there is sufficiently large motion in the vibration modes, and the method can also be used to monitor the variation of the damping ratio with time.

6. Conclusions

A procedure is proposed to identify the damping ratios of a structural system from measured accelerations based on the response sensitivity approach. Simulation results from a three-dimensional five-bay cantilever frame structure show that accurate results can be obtained which are robust to measurement noise and even with some model errors in the initial finite element model. Higher sampling rates and longer length of data in the identification are preferred for a more accurate set of results. The proposed method can also be used to monitor the variation of damping ratios in a structural system when moving windows of acceleration data are used in the identification. Measured data from a short duration and from a large group of sensors is preferable for the identification of a time-varying damping system.

Acknowledgment

The work described in this paper was supported by a grant from the Hong Kong Research Grant Council Project no. PolyU 5207/06E.

References

[1] L. Rayleigh, second ed., *Theory of Sound (two volumes)*, Dover Publications, New York, 1877 (Reissued 1945).
[2] D.J. Ewins, *Modal Testing: Theory and Practice*, Research Studies Press Ltd. (Wiley), Letchworth, England, 1984, pp. 153–180.
[3] F.L. Huang, X.M. Wang, Z.Q. Chen, X.H. He, Y.Q. Ni, A new approach to identification of structural damping ratios, *Journal of Sound and Vibration* 303 (1–2) (2007) 144–153.
[4] S.R. Ibrahim, A Time Domain Vibration Test Technique, PhD Thesis, Department of Mechanical Engineering, University of Calgary, Alberta, Canada, 1973.
[5] S.R. Ibrahim, E.C. Mikulcik, A method for the direct identification of vibration, *Shocked Vibration Bulletin* (Part 4), 1997.
[6] J.-N. Juang, R. Pappa, An eigensystem realization algorithm for modal parameter identification and model reduction, *AIAA Journal of Guidance, Control, and Dynamics* 8 (1985) 620–627.

[7] S.R. Ibrahim, An approach for reducing computational requirements in modal identification, *AIAA Journal* 24 (10) (1986).
[8] S.M. Batille, J.J. Hollkamp, Parameter identification of discrete-time series models for structural response prediction, *AIAA Journal* 27 (1989) 1636–1643.
[9] C. Gontier, M. Smail, P.E. Gauthier, A time domain method for the identification of dynamic parameters of structures, *Mechanical Systems and Signal Processing* 7 (1993) 45–56.
[10] S.R. Ibrahim, Random decrement technique for modal identification of structures, *Journal of Spacecraft and Rockets* 14 (11) (1997).
[11] M.E. Gaylard, Identification of proportional and other sorts of damping matrices using a weighted response-integral method, *Mechanical Systems and Signal Processing* 15 (2) (2001) 245–256.
[12] M. Ruzzene, A. Fasana, L. Garibaldi, B. Piombo, Natural frequencies and damping identification using wavelet transform: application to real data, *Mechanical Systems and Signal Processing* 11 (1997) 207–218.
[13] C.H. Lamarque, S. Penrot, A. Cuer, Damping identification in multi-degree-of-freedom systems via a wavelet-logarithmic decrement—part 1: theory, *Journal of Sound and Vibration* 235 (3) (2000) 361–374.
[14] A. Agneni, L. Balis-Crema, Damping measurements from truncated signals via Hilbert transform, *Mechanical Systems and Signal Processing* 3 (1989) 1–13.
[15] J. Chen, Y.L. Xu, R.C. Zhang, Modal parameter identification of Tsing Ma suspension bridge under Typhoon Victor: EMD-HT method, *Journal of Wind Engineering and Industrial Aerodynamics* 92 (2004) 805–827.
[16] J.S. Kang, S.K. Park, S.B. Shin, H.S. Lee, Structural system identification in time domain using measured acceleration, *Journal of Sound and Vibration* 288 (1–2) (2005) 215–234.
[17] S.B. Shin, S.H. Oh, Damage assessment of shear buildings by synchronous estimation of stiffness and damping using measured acceleration, *Smart Structures and Systems* 3 (3) (2007) 245–261.
[18] Z.R. Lu, S.S. Law, Features of dynamic response sensitivity and its application in damage detection, *Journal of Sound and Vibration* 303 (1–2) (2007) 305–329.
[19] N.W. Newmark, A method of computation for structural dynamics, *ASCE Journal of Engineering Mechanics Division* 85 (3) (1959) 67–94.
[20] S. Adhikari, J. Woodhouse, Identification of damping: part 1, viscous damping, *Journal of Sound and Vibration* 243 (1) (2001) 43–61.